Thermophotovoltaic and thermoelectric portable power generators

Walker R. Chan, Christopher M. Waits, John D. Joannopoulos, Ivan Celanovic

Walker R. Chan, Christopher M. Waits, John D. Joannopoulos, Ivan Celanovic, "Thermophotovoltaic and thermoelectric portable power generators," Proc. SPIE 9083, Micro- and Nanotechnology Sensors, Systems, and Applications VI, 90831W (4 June 2014); doi: 10.1117/12.2054173

SPIE.

Event: SPIE Defense + Security, 2014, Baltimore, Maryland, United States

Invited Paper

Thermophotovoltaic and Thermoelectric Portable Power Generators

Walker R. Chan[a], Christopher M. Waits[b], John D. Joannopoulos[a], and Ivan Celanovic[a]

[a]Massachusetts Institute of Technology, Cambridge, MA, USA

[b]Army Research Laboratory, Adelphi, MD, USA

ABSTRACT

The quest for developing clean, quiet, and portable high energy density, and ultra-compact power sources continues. Although batteries offer a well known solution, limits on the chemistry developed to date constrain the energy density to 0.2 kWh/kg, whereas many hydrocarbon fuels have energy densities closer to 13 kWh/kg. The fundamental challenge remains: how efficiently and robustly can these widely available chemical fuels be converted into electricity in a millimeter to centimeter scale systems? Here we explore two promising technologies for high energy density power generators: thermophotovoltaics (TPV) and thermoelectrics (TE). These heat to electricity conversion processes are appealing because they are fully static leading to quiet and robust operation, allow for multifuel operation due to the ease of generating heat, and offer high power densities. We will present some previous work done in the TPV and TE fields. In addition we will outline the common technological barriers facing both approaches, as well as outline the main differences. Performance for state of the art research generators will be compared as well as projections for future practically achievable systems. A viable TPV or TE power source for a ten watt for one week mission can be built from a >10% efficient device which is achievable with current state of the art technology such as photonic crystals or advanced TE materials.

Keywords: Portable power, thermophotovoltaics, thermoelectrics

1. INTRODUCTION

The ongoing proliferation of power intensive remote sensors, mobile systems, and portable devices has driven the development of increasingly compact, energy dense power sources. Rechargeable batteries represent a mature technology capable of providing energy densities of up to 100-300 Wh/kg, whereas hydrocarbon fuels have energy densities approaching 13 kWh/kg while promising rapid refueling. Thus, a generator with an efficiency of only a few percent will have the same energy density as the best lithium ion batteries. To this end, researchers have explored several possible energy conversion routes for providing next-generation portable power including mechanical heat engines, fuel cells, thermoelectrics, and thermophotovoltaics.[1] This work provides an overview of two thermal conversion processes: thermophotovoltaics and thermoelectrics, depicted schematically in Fig. 1. These heat to electricity conversion processes are appealing because they are fully static leading to quiet and robust operation, allow for multifuel operation due to the ease of generating heat, and offer high power densities.

Thermophotovoltaics (TPVs) is the conversion of heat to electricity by the thermal emission of photons and their subsequent absorption and conversion to electricity by infrared photovoltaic cells (TPV cells). The key challenge in designing a TPV system is matching the radiated spectrum to the conversion range of the TPV cells. Emission and absorption spectra can be seen in Fig. 2a. This may be accomplished with photonic crystals (PhCs), multilayer stacks, certain metals or rare earth elements, or with a filter on the cells. Because TPV systems rely on thermal radiation, the hot side tends to be around 800 to 1100°C although some systems run as high as 1500°C. The high temperatures make system engineering difficult primarily due to material stresses and degradation. Continued operation at high temperatures limits the emitter material to high temperature ceramics and low vapor pressure refractory metals to prevent evaporation and redeposition on the cells. Metallic PhCs offer tunable highly selective emission but rely on a nanostructured surface that can degrade under prolonged

Further author information: (Send correspondence to W.R.C.)
W.R.C: E-mail: wrchan@mit.edu

Micro- and Nanotechnology Sensors, Systems, and Applications VI, edited by Thomas George, M. Saif Islam, Achyut K. Dutta, Proc. of SPIE Vol. 9083, 90831W · © 2014 SPIE
CCC code: 0277-786X/14/$18 · doi: 10.1117/12.2054173

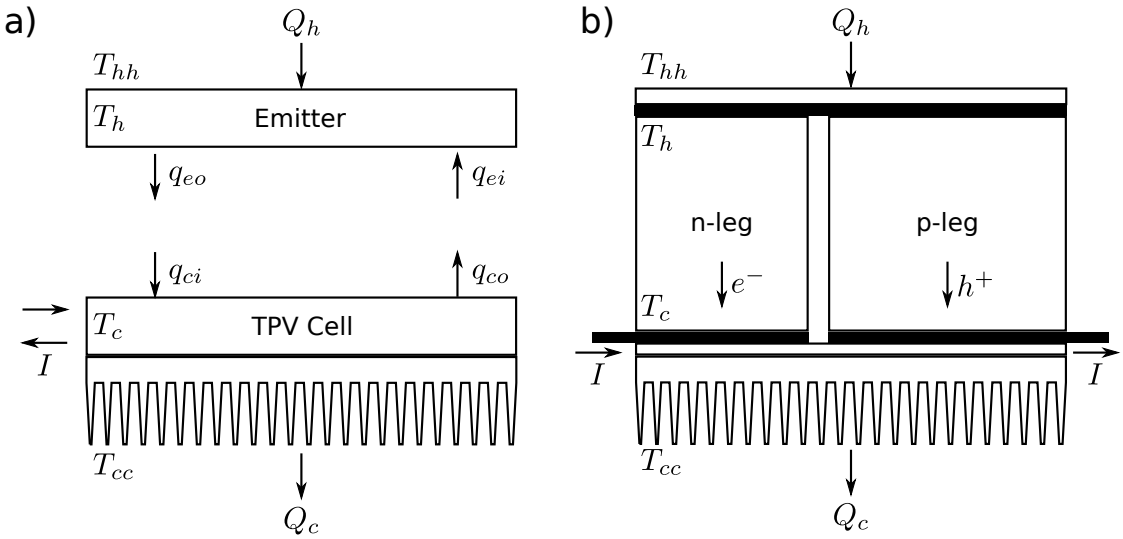

Figure 1: Schematic representations of TPV (a) and TE (b) devices.

Table 1: Experimental results in literature.

Technology	Temperature	Efficiency	Electric power	Power density	Note	Ref.
TE	115°C	1.5%	110 mW	70 mW/cm^2	extrapolated	9
TE	130°C	2.4%	300 mW	65 mW/cm^2		10
TE	270°C	2.5%	6 W	300 mW/cm^2		11
TE	582°C	2.4%	100 W	88 mW/cm^2	large system	12
TPV	740°C	1.6%	220 mW	110 mW/cm^2	pure oxygen	13
TPV	800°C	2.3%	344 mW	170 mW/cm^2	pure oxygen	13
TPV	1000°C	1.9%	13 W	300 mW/cm^2		14
TPV	1427°C	4.0%	50 W	100 mW/cm^2	preheated air	15

operation at high temperatures. Recently, a thermal barrier coating was demonstrated to protect a Tantalum (Ta) PhC from degradation due to surface diffusion and surface contamination.[2]

Thermoelectrics (TEs) convert heat to electricity by the thermal diffusion of charge carriers. The key challenge is engineering the TE materials themselves. The materials must have the conflicting properties of high electrical conductivity and low thermal conductivity. This is achieved by creating a complex crystallographic unit cell or through nanostructuring. Typical materials are Bi_2Te_3 or alloys of Sb_2Te_3 and Bi_2Se_3 for temperatures up to 200-300°C, PbTe, TAGS, and skutterudites for medium temperatures up to 600°C, and SiGe for high temperatures up to 1000°C.[3] A commonly used figure of merit for thermoelectric materials is $zT = \alpha^2 T/\rho\kappa$ where α is the Seebeck coefficient, ρ is the electrical resistivity, κ is thermal conductivity, and T is the temperature. Typical material zT values are shown in Fig. 2b. Higher temperatures can lead to improved performance but stress materials and make system engineering more difficult. High thermal conductivity joints between the heterogeneous materials comprising the TE stack (the n- and p-type TE materials, electrical interconnects, electrical isolation, and the heat source), thermal isolation, and thermal expansion mismatches make device integration difficult.[4,5] Additionally, the thermoelectric materials themselves are susceptible to oxidation and sublimation.[6,7] For high temperatures, segmented TEs may be used to maximize device performance over then entire temperature range.[8]

Low temperature TE systems have been built around propane- or butane-air MEMS microburners and Bi_2Te_3 thermoelectrics.[10,11] A larger, medium temperature system was also built using PbTe/ZnSb themoelectrics.[12] One TPV system used propane-oxygen combustion in a silicon MEMS microburner to heat an integrated silicon/silicon dioxide multilayer selective emitter which was tuned to match the InGaAsSb (2.3 µm bandgap) cells.[13] The system was limited to 2.3% efficiency because material incompatibilities prevented operation above

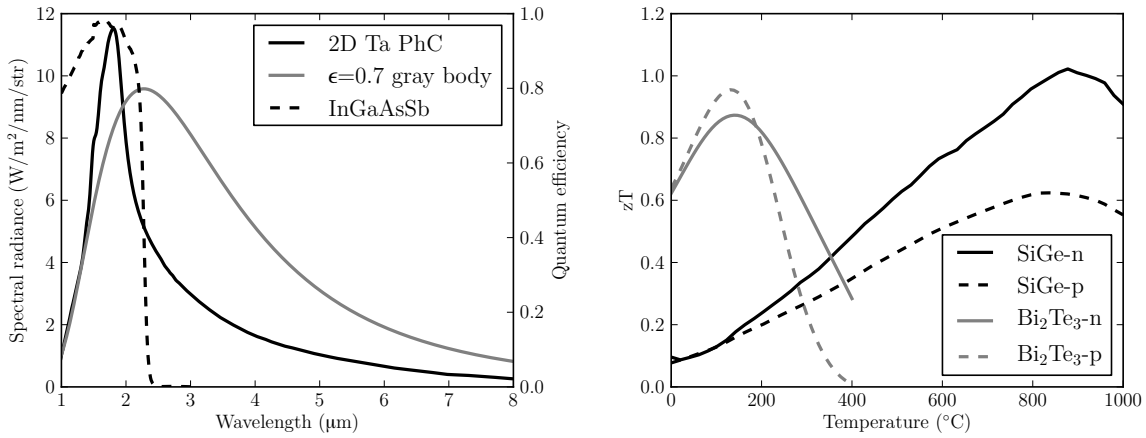

(a) TPV (b) TE

Figure 2: Data used for both TPV (a) and TE (b) models.[11,20–23] The spectra in (a) are at 1000°C.

800°C.[16] A larger TPV system used propane-air combustion to heat a dielectric coated platinum emitter matched to GaSb cells, for an efficiency of 1.9%.[14] A large-scale TPV system (50 W_e) was built using a rare earth doped ceramic emitter matched to silicon cells.[15] These systems are summarized in Table 1.

Harnessing the high energy density of hydrocarbon fuels on a millimeter scale is not easy. The systems described in Table 1 which could be considered portable are all around 2-3% efficient. Those system efficiencies are not high enough to warrant the added cost and complexity versus a battery. Furthermore, many of the systems have glaring impracticalities such as the use of hydrogen or oxygen or balance of plant omissions such as chilled water cooling systems or externally preheated combustion air. Is there something fundamentally wrong with these thermal conversion processes? Modeling work indicates that the poor performance is not fundamental. In this work we predict 12% device efficiency, and other predict even higher.[17–19] The shortcomings in the system demonstrations are twofold: the systems do not incorporate the best materials and latest technologies that tend to be cited when modeling, and are not optimized on a system level due to practical constrains on fabrication and availability of specialized materials.[11,13]

In the following sections, we will model state of the art TPV and TE devices. Based on those results, we will optimize TPV and TE systems consisting of a burner, TPV or TE device, and heat sink. The system models will be used to compare the performance of state of the art TPV and TE generators against those that are achievable today and lithium batteries.

2. THERMOPHOTOVOLTAIC MODEL

For the TPV system, we analyzed an emitter-cell pair separated by a small vacuum gap as shown in Fig. 1(a). The emitter has a wavelength dependent emissivity $\epsilon_e(\lambda)$ and is at temperature T_h. The total heat flux into the emitter, Q_h, can be found by integrating the radiated spectrum. Furthermore, the spectrum incident on the cell can be found by a detailed energy balance of optical cavity consisting of an emitter and TPV cell:

$$q_{ci}(\lambda) = \frac{F\epsilon_e}{(1-\rho_c)(1-\rho_e F^2) - \rho_c\rho_e F^2} e_b(\lambda, T_h), \tag{1}$$

where $e_b(\lambda, T_h)$ is the blackbody spectrum of an emitter at temperature T_h, ρ is reflectance, and ϵ is emittance. The subscripts refer to the components of the system: e for emitter and c for cell.[24] In the derivation, it is assumed that the emitter is the only component that radiates and that all reflections and emissions are purely diffuse. F is the geometric view factor between the emitter and the cell.

The photocurrent generated in the cell can be found by

$$I_{ph} = eF \int_0^\infty \frac{\lambda}{hc} q_{ci}(\lambda)\eta_E(\lambda)d\lambda, \tag{2}$$

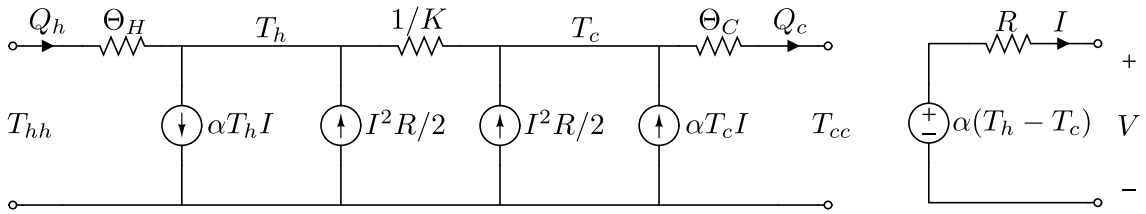

Figure 3: Thermal and electrical equivalent circuit models for a thermoelectric system.

where $q_{ci}(\lambda)$ is the radiated power per unit wavelength incident on the cell, hc/λ is the photon energy, $\eta_E(\lambda)$ is the external quantum efficiency, and e is the electron charge. The TPV cell itself was modeled with a single diode equivalent circuit model with temperature dependent parameters. The circuit model is described by

$$I = I_{ph} - I_0 \left(\exp\left[\frac{q}{nk_B T_c}(V + IR_s) \right] - 1 \right) - \frac{V + IR_s}{R_{sh}}, \tag{3}$$

where I and V are the terminal current and voltage, $q/k_B T_c$ is the thermal voltage, I_{ph} is the photocurrent, I_0 is the diode dark current, n is the diode ideality factor, and R_s and R_{sh} are the shunt and series resistances.[20] The electrical power output of the cell is taken at the maximum power point.

The heat flux out the heat sink, Q_c, is the total radiant heat reaching the cell less the electrical power output. It is assumed that the heat sink adds a thermal resistance Θ_C between the junction temperature, T_c, and the ambient temperature, T_{cc}. The junction temperature is used in modeling the electrical properties of the TPV cell.[20]

The peak efficiency for a InGaAsSb[25,26] TPV device is around 6% for a greybody emitter and around 12% for a PhC emitter[21,22] at nearly 1200°C (for both). We assume a heat sink thermal resistance of $\Theta_C = 2$ °C/W between the InGaAsSb cells and the $T_{cc} = 20$°C ambient. The spectral properties of the emitters and cells are shown in Fig. 2a. Further improvements to the Ta PhC-InGaAsSb device efficiency are relatively simply accomplished by reducing long wavelength radiation or incorporating a filter onto the cell side to recycle the long wavelength radiation.[17]

3. THERMOELECTRIC MODEL

We analyzed the thermoelectric pair shown in Fig. 1(b). The n- and p-legs have Seebeck coefficient α, electrical resistivity ρ, and thermal conductivity κ. The device has a total Seebeck coefficient, thermal conductivity, and electrical resistivity of

$$\alpha = \alpha_p - \alpha_n \tag{4}$$

$$K = \kappa_n \frac{A_n}{l} + \kappa_p \frac{A_p}{l} \tag{5}$$

$$R = \rho_n \frac{l}{A_n} + \rho_p \frac{l}{A_p} \tag{6}$$

where the material propertie(α, ρ, and κ) of the individual legs are denoted with n and p subscripts.[27,28] Thus, the figure of merit for the entire device is $ZT = \alpha^2 T/KR$ (upper case Z is used for devices, lower case z is used for materials). Furthermore, the material properties (α, ρ, κ) are temperature dependent. In a device, the temperature varies along the length of the leg, meaning that the material properties also vary. The true device properties should be found by integrating along the length of the leg. Alternatively, the device properties can be approximated by using an effective temperature.

If one side of the TE device is heated and the other is cooled, an open circuit voltage $V = \alpha(T_h - T_c)$ develops at the terminals, where T_h and T_c are the hot and cold side temperatures. The heat flux into and out of a TE device is the sum of the Peltier effect, Joule heating, and thermal conduction,

$$Q_h = -\alpha T_h I + I^2 R/2 - K(T_h - T_c) \tag{7}$$

$$Q_c = \alpha T_c I + I^2 R/2 + K(T_h - T_c). \tag{8}$$

Table 2: TE and TPV systems designs to supply 10 W for 168 hours. Li-ion battery is shown for comparison.

	TE: SiGe	TPV: Ta PhC	TE: Bi_2Te_3	TPV: greybody	Li-ion
Burner temperature T_{hh}	870°C	1130°C	210°C	1180°C	
Cold side temperature T_c	110°C	58°C	65°C	95°C	
System efficiency	6.1%	5.6%	4.6%	2.4%	
Device efficiency	9.9%	11.6%	4.9%	5.3%	
Device power density	610 mW/cm^2	790 mW/cm^2	120 mW/cm^2	940 mW/cm^2	
Fuel mass	2100 g	2300 g	2800 g	5400 g	
Device mass	270 g	12 g	270 g	10 g	
Heat sink mass	140 g	320 g	440 g	390 g	
System mass	2500 g	2600 g	3500 g	5800 g	12000 g
System energy density	660 Whr/kg	630 Whr/kg	470 Whr/kg	270 Whr/kg	140 Whr/kg

where I is the current at the terminals of the device.[27,28] The thermal circuit is shown in Fig. 3. The circuit includes two additional thermal resistances Θ_H which represents the thermal resistance between the heat source and the TE legs (bus bars, electrical insulation, etc.) and Θ_C which represents primarily the heat sink. From an electrical perspective, the equivalent circuit is shown in Fig. 3. We assume that the load resistance is equal to R to maximize electrical power output.

Additionally, the legs have areas A_n and A_p which sum to 1 cm^2 and a common length l. The length and areas were numerically optimized to maximize the product of the power density and efficiency. When the device is optimized according to the above criterion, the peak efficiency for a Bi_2Te_3 device is a little over 6% at a hot side temperature of around 300°C. Peak efficiency for a SiGe device is 9% at a hot side temperature of 800°C. Once again, we assume a heat sink thermal resistance of $\Theta_C = 2$ °C/W between the cold side of the TE and the $T_{cc} = 20$°C ambient.

4. SYSTEM MODEL

We have modeled TPV and TE device performance but we are actually interested in the performance of a complete system capable of supplying a given electrical power for a given amount of time, in this case ten watts for one week. The system is defined as the fuel, the TPV or TE device, and a naturally cooled heat sink. The figure of merit used to evaluate the system is the system energy density which is a composite of (1) the efficiency which determines the fuel mass, (2) the power density which determines the device mass, and (3) the temperature dependence of efficiency and power density which determines the heat sink mass. The optimal system design depends on the specific mission. For example, a larger heat sink lowers the cold side temperature which increases efficiency. On a long mission, it would be better to carry a big heat sink and less fuel. On a short mission, it would be better to carry a small heat sink and more fuel.

The TE or TPV device is modeled as described in the previous sections. For each technology, we modeled two devices, one based on readily available materials and one based on state of the art materials, shown in Fig. 2. For TPV, we used InGaAsSb cells[25,26] and both an $\epsilon = 0.7$ greybody emitter and the latest Ta PhC emitter.[21,22] For TE, we used both low temperature Bi_2Te_3[11] and high temperature SiGe.[23] We included the mass of the device to prevent the optimization code from increasing efficiency at the expense of power density. We assume that density of a TE device is 3 g/cm^3 and the volume is calculated from the active area dimensions and leg lengths. The density of the TPV device is taken to be 1 g/cm^2.[13,16]

The burner converts the caloric content of the fuel to heat. The fuel is burned with a stoichiometric amount of air that has been preheated to half the hot side temperature, to simulate the effect of a recuperator. The heat carried out by the exhaust is the only heat loss included in the model except those inherent to the device. We assume that the fuel has a heating value of 46 MJ/kg which covers propane, butane, gasoline, JP-8, and most other hydrocarbons.

The heat sink rejects heat from the cold side of the device to the ambient, and is cooled with natural convection, where its thermal conductivity is assumed to scale with mass according to a power law. The size of

the heat sink influences device efficiency by changing the cold side temperature. For TE, T_c appears directly in the device model. For TPV, T_c affects the TPV cell properties. We could have added another dimension to the problem by allowing for active cooling.[29]

All four designs were optimized numerically with total mass as the figure of merit. The TPV systems had hot side temperature and heat sink size as the free parameters. The TE systems had hot side temperature, heat sink size, and leg dimensions as free parameters. The optimization results are shown in Table 2.

We modeled two TPV systems: one with a greybody emitter and InGaAsSb cells and a second with a Ta PhC emitter and InGaAsSb cells. The greybody system has a relatively low energy density due primarily to the spectral low efficiency. The low spectral efficiency also causes a large amount of waste heat in the cells, requiring a large heat sink. The PhC system has 2.5 times the energy density because (1) the PhC reduces heat loss from the emitter, (2) the PhC's emission approaches blackbody at short wavelengths which improves the power density, and (3) the reduced long wavelength emission reduces the amount of waste heat that must be removed from the cell.

We modeled two TE systems: one with a SiGe device and on with Bi_2Te_3. The Bi_2Te_3 system outperforms the greybody TPV system despite lower device performance. The TPV device runs much hotter than the TE device, resulting in a much larger heat loss out the exhaust of the burner. The performance of the SiGe system is on par with the PhC TPV system, despite the device efficiency being lower. The reason, once again, is that the TE system operates at a lower temperature and has small heat loss from the burner.

In the system model, we only included the device, fuel, and heat sink in the system mass and ignored the fuel tank, device packaging, recuperator, interconnects, housings, and balance of plant components. The fuel tank could add 10% of the weight of the fuel for liquid fuels and more weight for propane/butane. The recuperator weight was not included in this work but could become important in comparing TPV and TE, especially Bi_2Te_3, due to the different temperatures. The mass of balance of plant components (pumps, fans, etc.) can easily be 50 g. Thus, the system weight could be perhaps 20% higher when these necessary components are included. Nevertheless, the top TPV and TE systems would be around the 500 Whr/kg mark, still double that of primary batteries and more than 3 times better than rechargeables.

5. CONCLUSION

This work provided an overview of two thermal conversion processes, TPV and TE, as potential next generation portable power sources that could harness the high energy density of hydrocarbon fuels. These heat to electricity conversion processes are appealing because they are fully static leading to quiet and robust operation, allow for multifuel operation due to the ease of generating heat, and offer high power densities. We developed semi-analytic system level models for both TPV and TE. From the system models, we conclude that a viable TPV or TE power source for a ten watt for one week mission can be built from a >10% efficient device. Fortunately, that is achievable with current state of the art technology such as PhCs or advanced TE materials. Of course demonstrating an energy density of 600-700 Whr/kg experimentally would be a considerable engineering challenge. The device and the heat sink are 10-20% of the total system mass and are oftentimes overlooked on a device level where efficiency is the sole figure of merit. Device weight is determined by the power density. Heat sink weight is determined by the device's ability to maintain efficiency at elevated cold side temperatures. Additionally, a hotter hot side temperature oftentimes enables a higher device efficiency but not necessarily a higher system efficiency due to increased heat loss. We suspect that some of these challenges may be relatively easy ways to improve system efficiency compared to research on individual components.

ACKNOWLEDGMENTS

This work was partially supported by the Army Research Office through the Institute for Soldier Nanotechnologies under Contract Nos. DAAD-19-02-D0002 and W911NF-07-D0004. WRC was partially supported by the MIT S3TEC Energy Research Frontier Center of the Department of Energy under Grant No. DE-SC0001299.

REFERENCES

[1] Mitsos, A., [*Microfabricated power generation devices : design and technology*], Wiley-VCH, Weinheim (2009).

[2] Rinnerbauer, V., Yeng, Y. X., Chan, W. R., Senkevich, J. J., Joannopoulos, J. D., Soljačić, M., and Celanovic, I., "High-temperature stability and selective thermal emission of polycrystalline tantalum photonic crystals," *Opt. Express* **21**, 11482–11491 (May 2013).

[3] Snyder, G. J. and Toberer, E. S., "Complex thermoelectric materials," *Nature Materials* **7**, 105–114 (Feb 2008).

[4] Caillat, T., "Thermoelectrics for space applications: Past, present and future." MIT S3TEC Seminar (Nov 2013).

[5] Gao, Y., Marconnet, A., Panzer, M., LeBlanc, S., Dogbe, S., Ezzahri, Y., Shakouri, A., and Goodson, K., "Nanostructured interfaces for thermoelectrics," *Journal of Electronic Materials* **39**(9), 1456–1462 (2010).

[6] Nesbitt, J. A., Opila, E. J., and Nathal, M. V., "Insitu growth of a Yb_2O_3 layer for sublimation suppression for $Yb_{14}MnSb_{11}$ thermoelectric material for space power applications," *Journal of Electronic Materials* **41**(6), 1267–1273 (2012).

[7] Zhao, D., Tian, C., Liu, Y., Zhan, C., and Chen, L., "High temperature sublimation behavior of antimony in $CoSb_3$ thermoelectric material during thermal duration test," *Journal of Alloys and Compounds* **509**(6), 3166 – 3171 (2011).

[8] Snyder, G. J., "Design and optimization of compatible, segmented thermoelectric generators," in [*Twenty-second International Conference on Thermoelectrics*], 443 (2003).

[9] Vican, J., Gajdeczko, B., Dryer, F., Milius, D., Aksay, I., and Yetter, R., "Development of a microreactor as a thermal source for microelectromechanical systems power generation," *Proceedings of the Combustion Institute* **29**(1), 909 – 916 (2002). Proceedings of the Combustion Institute.

[10] Yoshida, K., Tanaka, S., Tomonari, S., Satoh, D., and Esashi, M., "High-energy density miniature thermoelectric generator using catalytic combustion," *J. Microelectromech. Syst.* **15**, 195–203 (2006).

[11] Marton, C. H., Haldeman, G. S., and Jensen, K. F., "Portable thermoelectric power generator based on a microfabricated silicon combustor with low resistance to flow," *Industrial & Engineering Chemistry Research* **50**(14), 8468–8475 (2011).

[12] Corry, T. M., Moreland, W. C., and Strickland, E. L., "Design of a 100-watt thermoelectric generator," *Electrical Engineering* **79**, 482–488 (June 1960).

[13] Chan, W. R., Bermel, P., Pilawa-Podgurski, R. C. N., Marton, C. H., Jensen, K. F., Senkevich, J. J., Joannopoulos, J. D., Soljacic, M., and Celanovic, I., "Toward high-energy-density, high-efficiency, and moderate-temperature chip-scale thermophotovoltaics," *Proceedings of the National Academy of Sciences* **110**(14), 5309–5314 (2013).

[14] Doyle, E., Shukla, K., and Metcalfe, C., "Development and demonstration of a 25 watt thermophotovoltaic power source for a hybrid power system," Tech. Rep. TR04-2001, National Aeronautics and Space Administration (August 2001).

[15] Bitnar, B., Durisch, W., and Holzner, R., "Thermophotovoltaics on the move to applications," *Applied Energy* **105**(0), 430 – 438 (2013).

[16] Chan, W. R., Wilhite, B. A., Senkevich, J. J., Soljacic, M., Joannopoulos, J., and Celanovic, I., "An all-metallic microburner for a millimeter-scale thermophotovoltaic generator," *Journal of Physics: Conference Series* **476**(1), 012017 (2013).

[17] Yeng, Y. X., Chan, W. R., Rinnerbauer, V., Joannopoulos, J. D., Soljačić, M., and Celanovic, I., "Performance analysis of experimentally viable photonic crystal enhanced thermophotovoltaic systems," *Opt. Express* **21**, A1035–A1051 (Nov 2013).

[18] Zenker, M., Heinzel, A., Stollwerck, G., Ferber, J., and Luther, J., "Efficiency and power density potential of combustion-driven thermophotovoltaic systems using gasb photovoltaic cells," *Electron Devices, IEEE Transactions on* **48**, 367–376 (Feb 2001).

[19] Biswas, K., He, J., Blum, I. D., Wu, C.-I., Hogan, T. P., Seidman, D. N., Dravid, V. P., and Kanatzidis, M. G., "High-performance bulk thermoelectrics with all-scale hierarchical architectures," *Nature* **489**(7416), 414–418 (2012).

[20] Chan, W. R., Huang, R., Wang, C. A., Kassakian, J., Joannopoulos, J. D., and Celanovic, I., "Modeling low-bandgap thermophotovoltaic diodes for high-efficiency portable power generators," *Sol. Energy Mater. Sol. Cells* **94**, 509–514 (2010).

[21] Stelmakh, V., Rinnerbauer, V., Geil, R. D., Aimone, P. R., Senkevich, J. J., Joannopoulos, J. D., Soljacic, M., and Celanovic, I., "High-temperature tantalum tungsten alloy photonic crystals: Stability, optical properties, and fabrication," *Applied Physics Letters* **103**(12), 123903 (2013).

[22] Rinnerbauer, V., Ndao, S., Xiang Yeng, Y., Senkevich, J. J., Jensen, K. F., Joannopoulos, J. D., Soljacic, M., Celanovic, I., and Geil, R. D., "Large-area fabrication of high aspect ratio tantalum photonic crystals for high-temperature selective emitters," *Journal of Vacuum Science Technology B: Microelectronics and Nanometer Structures* **31**(1), 011802–011802–7 (2013).

[23] Vining, C. B., Laskow, W., Hanson, J. O., Van der Beck, R. R., and Gorsuch, P. D., "Thermoelectric properties of pressure sintered $Si_{0.8}Ge_{0.2}$ thermoelectric alloys," *Journal of Applied Physics* **69**(8), 4333–4340 (1991).

[24] Chubb, D. L., [*Fundamentals of Thermophotovoltaics*], Elsevier (2007).

[25] Wang, C. A., Choi, H. K., Ransom, S. L., Charache, G. W., Danielson, L. R., and DePoy, D. M., "High-quantum-efficiency 0.5eV GaInAsSb/GaSb thermophotovoltaic devices," *Applied Physics Letters* **75**(9), 1305–1307 (1999).

[26] Dashiell, M. W., Beausang, J. F., Ehsani, H., Nichols, G. J., Depoy, D. M., Danielson, L. R., Talamo, P., Rahner, K. D., Brown, E. J., Burger, S. R., Fourspring, P. M., Jr., W. F. T., Baldasaro, P. F., Wang, C. A., Huang, R. K., Connors, M. K., Turner, G. W., Shellenbarger, Z. A., Taylor, G., Li, J., Martinelli, R., Donetski, D., Anikeev, S., Belenky, G. L., and Luryi, S., "Quaternary InGaAsSb thermophotovoltaic diodes," *Electron Devices, IEEE Transactions on* **53**, 2879–2891 (Dec. 2006).

[27] Min, G. and Rowe, D., "Peltier devices as generators," in [*CRC Handbook of Thermoelectrics*], Rowe, D., ed., CRC Press, Boca Raton (1995).

[28] Cobble, M. H., "Calculation of generator performance," in [*CRC Handbook of Thermoelectrics*], Rowe, D., ed., CRC Press, Boca Raton (1995).

[29] Heymann, D. B., Meyer, C. D., Jankowski, N. R., and Morgan, B. C., "Modeling the system impact of cooling performance on a compact thermoelectric generator," in [*PowerMEMS 2009*], 601–604 (2009).